Tethys, 6, 3–14, 2009
Journal of Weather & Climate of the Western Mediterranean
www.tethys.cat
ISSN-1697-1523
eISSN-1139-3394
DOI:10.3369/tethys.2009.6.01

Journal edited by **ACAM**
(Associació Catalana de Meteorologia)

Climatic study of the exponent "n" in IDF curves: application for the Iberian Peninsula

R. Moncho[1], F. Belda[2] and V. Caselles[3]

[1]Unit of Marine Research. AZTI-Tecnalia
[2]Territorial Delegation in Murcia. AEMET
[3]Department of Earth Physics and Thermodynamics. Universitat de València

Received: 4-IX-2008 – Accepted: 10-XII-2008 – **Translated version**

Correspondence to: rmoncho@azti.es

Abstract

The analysis of maximum precipitation is usually carried out by using IDF curves (Intensity-Duration-Frequency), which in turn could be expressed as MAI curves (Maximum Average Intensities). An index "n" has been developed in this work, defined from the exponent obtained when adjusting IDF climatic curves to MAI curves. That index provides information about how maximum precipitation is achieved in a certain climatic area, according to the relative temporal distribution of maximum intensities. From the climatic analysis of index "n", large areas could be distinguished in the Iberian Peninsula, characterized by rain maxima of a stormier origin (peninsular inland), and areas characterized by rain maxima of a more frontal origin (southwest, Atlantic coast and Mediterranean coast). Additionally, these areas could be more specifically divided according to the persistence of maximum precipitation.

Key words: precipitation intensity, IDF curves, MAI curves, regularity index

1 Introduction

The patterns of intense precipitation are one of the possible variables that are sensitive to climate change. In fact, rain intensity, in addition to depending on the content of precipitable water in the atmosphere, also depends on the vertical thermal gradient in the different precipitating cloud systems. Different organizations are observing changes in global temperature in various atmosphere layers between the surface and the stratosphere (NASA, 2008; NOAA, 2008).

Therefore, variations in the behavior of maximum intensities can be expected. Such variations will be determined by two factors: the natural and intrinsic variability of a climate and the variation of the averages of the given climate.

As a preamble to a possible study of the variation of intensity patterns, the following work proposes a way of analyzing the natural variability of the maximum intensities of a climate.

The goal is to identify and quantify the general characteristics of the climatic patterns of intense precipitation based on a model of temporal distribution of the Maximum Average Intensities of precipitation. That is to say, we intend to characterize cases of extreme precipitation according to their temporal distribution, if they are more similar to storms (precipitation concentrated in "short periods of time") or if they are more similar to fronts (regular precipitation with regard to "long periods of time"). Such a distribution model is applied to precipitation isolated in time as occasional showers, and it attempts to quantify this regularity of convective-advective precipitation in the field of meteorology. However, we will prove that it can be extended to be applied to climatology by using IDF curves.

2 Methodology

2.1 Curves of Maximum Average Intensities

The main magnitude that is going to be used in this work is the Maximum Average Intensity, I, which is the quotient between the maximum accumulation in a certain period of time, $P_{max}(t)$, and the mentioned period of time, t:

$$I(t) = \frac{P_{max}(t)}{t} \quad (1)$$

Table 1. Classification of rainfall according to the regularity of intensity.

n	Kind of curve	Intensity	Temporal distribution
0.00 - 0.20	Very gentle	Practically constant	Very regular
0.20 - 0.40	Gentle	Lightly variable	Regular
0.40 - 0.60	Normal	Variable	Irregular
0.60 - 0.80	Pronounced	Moderately variable	Very irregular
0.80 - 1.00	Very pronounced	Strongly variable	Nearly instantaneous

The relative distribution of the Maximum Average Intensities (MAI) of precipitation, in relation to the averaging time, is approximated by depending only on the exponent n in the following curve (see Annex A),

$$I(t) = I_0(t_0)\left(\frac{t_0}{t}\right)^n \tag{2}$$

where I is the MAI in a period of time t, I_0 is the MAI in a reference period of time t_0, and n is an adimensional parameter adjustable to the data. We note that the expression is invariable before the change of units and before the changes in the reference intensity $I_0(t_0)$.

Thus, to classify precipitation quantitatively, we will need three theoretical values:

- Any Maximum Average Intensity of reference $I_0(t_0)$,
- The duration of the shower related to a relative maximum of intensity t,
- The variability of the intensity, according to the value of the exponent n.

We want to classify the precipitation according to the variability of the intensity, and therefore we will pay attention to the exponent of the Maximum Average Intensity curve (see Table 1).

This classification criterion is independent of the absolute maximum intensity, so that it is focused on describing the variability of the intensity of the precipitation, and it can have values between 0 and 1, both excluded, of both a constant and highly variable intensity.

As its principal innovation, this work proposes the use of this model to analyze the temporal distribution of the maximum climatic precipitation in the peninsular Spain in detail. Therefore, we will have to combine it with other models that refer to the frequency of occurrences of given cases of intense precipitation.

2.2 Intensity-Duration-Frequency curves

The Intensity-Duration-Frequency (IDF) curves are the result of connecting the representative points of the average precipitation intensity in intervals of different duration, all corresponding to the same frequency or return period (Témez, 1978), thus, making it possible to analyze the changes of the curve in relation to that return period. To carry this out, we can take any direction and analyze the cut-off intensity in all IDF curves, that is, which average intensity values are expected for the same duration in each return period.

Therefore, the maximum precipitation expected Y, for a determined duration t, will be determined depending on the return period p. One of the simplest expressions that describe this dependence is expressed by the Gumbel law:

$$F(Y) = \exp[-\exp(-\alpha(Y-u))] \tag{3}$$

where *F(Y)* is the probability of exceeding a precipitation *Y(p)* of a certain return period p, while α and u are adjustable parameters. For a return period p much larger than a year, we find the solution,

$$F(Y) = 1 - \frac{1}{p} \tag{4}$$

where p is the return period expressed in years.

From Equations 3 and 4, we obtain that the expected maximum precipitation for a return period p is:

$$Y(p) = u - \frac{1}{\alpha}\ln\left[-\ln\left(1-\frac{1}{p}\right)\right] \approx u + \frac{1}{\alpha}\ln p = \\ = k + \frac{1}{\alpha}\ln\frac{p}{p_0} \tag{5}$$

where k is the result of a redefinition of constants such as $k = u + \frac{\ln p_0}{\alpha}$.

Another mathematical relation frequently used to describe the implicit function between precipitation and return period is the one used by Etoh et al. (1986), known as SQRT-ET$_{max}$,

$$F(Y) = \exp\left[-\kappa\left(1+\sqrt{\beta Y}\right)\exp\left(-\sqrt{\beta Y}\right)\right] \tag{6}$$

where κ and β are adjustable parameters. This expression could also be developed and approximated using the solution of Equation 4, in the same way as Equation 5. In general, for normalized return periods in which p/p_0 is between 1 and 100, the result is approximately:

$$Y(p) \approx (s^2 - 4.12) + (2s + 4.65)\frac{1}{0.756\sqrt{\beta}}\ln\frac{p}{p_0} \tag{7}$$

where $s \equiv \left(\frac{\ln\kappa + \ln p_0 + 0.135}{0.756\sqrt{\beta}}\right)$.

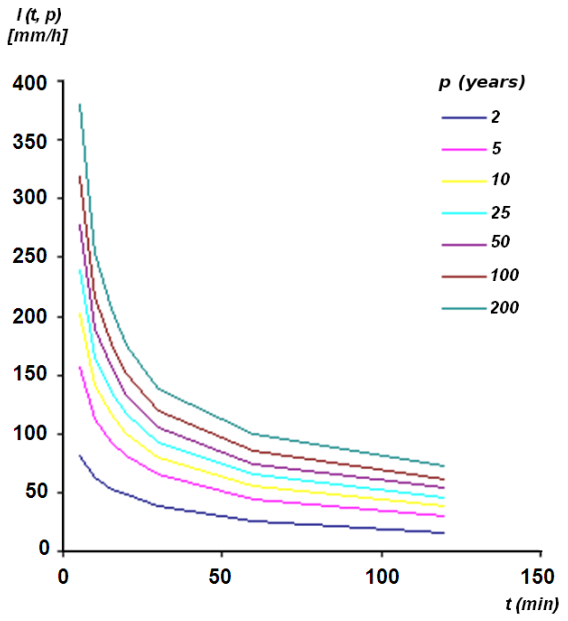

Figure 1. IDF curves in València, *I(t,p)*, where p represents the return period in years and t the duration in minutes.

2.3 Combination of MAI curves and IDF curves

The central method used in this work is mainly based on the adjustment of IDF curves (Intensity-Duration-Frequency) to MAI curves (Maximum Average Intensities). This is possible because each IDF curve represents a temporal distribution of the Maximum Average Intensities associated to a certain return period.

Thus, by using an adequate nomenclature of the variables, we find that IDF curves have to be equivalent to Equation 2, to which we add the dependence with the return period:

$$I(t,p) = I(t_0,p)\left(\frac{t_0}{t}\right)^{n(p)} \tag{8}$$

where *I(t,p)* is the corresponding intensity to a IDF curve of partial duration t, return period p and reference intensity $I_0(t_0,p)$, which corresponds to the average precipitation during t_0 minutes, that is to say P_0/t_0.

Therefore, we will use Equation 8 throughout this work to represent the temporal dependence of the intensity of precipitation; thus, one of the objectives is to find the mathematical expressions that represent the dependence of the reference intensity I_o, and of the index n with the return period, p.

We underscore that the innovation in this work is the characterization of the climatology of IDF curves through the adimensional parameter, *n(p)*, which represents the relative temporal distribution in Equation 8. It is worth noting, nevertheless, that in the final references we can find other empirical models very similar to Equation 8, cited in Pereyra-Díaz et al. (2004) and Ghahraman and Hoss Eini (2005), about the temporal distribution of IDF curves; we recover, for instance, the expression of Besson (Remenieras, 1970), Equation 9, that of Sherman (1931), Equation 10, and Chow (1962) expression, Equation 11:

$$I = \frac{a}{t+b} \tag{9}$$

$$I = \frac{a}{(t+b)^c} \tag{10}$$

$$I = \frac{a}{t^c+b} \tag{11}$$

where I is the corresponding intensity to an IDF curve of partial duration t, while a, b and c are empirically adjustable parameters. Notice that if $b = 0$ in Equation 10 and Equation 11, the result is Equation 8.

In other words, in Equation 8 we only find two parameters for each return period: the most important parameter, as mentioned before, is n, which is independent of time (Moncho, 2008); and the other parameter is the reference intensity $I(t_o)$, which could be adjusted with all intensities, or take any of them.

Other works about the temporal dependence of IDF curves in the Iberian Peninsula are those of the M.O.P.U. (1990) and Ferrer (1996), where we find that the Maximum Average Intensity in a time t is given by the expression:

$$I(t,p_0) = I(1d,p_0)\left[\frac{I(1h,p_0)}{I(1d,p_0)}\right]^{3.529-2.529t^{0.1}} \tag{12}$$

where $I(t,p_0)$ is the Maximum Average Intensity in t hours, while $I(1h,p_0)$ is the Maximum Average Intensity in one hour, and $I(1d,p_0)$ is the maximum intensity in one day.

3 Results

3.1 Study of a particular case: IDF curves in València

We have the data of the IDF curves in València (AEMET, 2003), indicated in Table 2 and represented in Figure 1, which were calculated using SQRT-ET$_{max}$. Such data have been adjusted to the corresponding MAI curves in order to infer the exponent n associated to each return period, p.

IDF curves, as any other Maximum Average Intensity curves (MAI), follow the Equation 2, where *I(t)* is the Maximum Average Intensity corresponding to t minutes, and *I(t_0)* is the reference intensity to t_0 minutes. For the sake of convenience, we will choose as time of reference t_0 = 60 minutes, although this does not affect the shape of *I(t)* due to the mathematical properties of this expression. Therefore, Table 3 is the result of adjusting the data in València to Equation 2 for each return period.

By definition IDF curves depend on the return period, that is to say *I(t) = I(t,p)*, as a consequence *n = n(p)* and also

Table 2. IDF data of València, Intensity *I(t,p)* (mm h^{-1}), where p represents the return period in years and t the duration in minutes.

Duration	p, Return period (years)							
(minutes)	2	5	10	25	50	100	200	500
5	81	124	156	202	239	278	319	380
10	63	91	112	141	165	189	216	253
15	53	76	93	117	135	156	177	206
20	48	67	81	100	117	133	151	175
30	39	54	65	80	93	105	119	138
60	25.3	36.2	44.3	55.7	65	74.4	84.8	99.6
120	16.2	24.3	30.4	39	45.9	53.7	61.5	72.9
180	12.6	19.3	24.3	31.5	37.4	43.6	50.2	59.6
360	8.2	12.8	16.4	21.4	25.3	29.8	34.5	40.8
720	5	7.7	9.8	12.8	15.2	17.8	20.6	24.5

Table 3. IDF curves adjustment to MAI curves, according to the return period for the data for València.

p	n	*I(t_0)*	R^2
2	0.573	23.4	0.990
5	0.558	34.5	0.995
10	0.550	42.9	0.997
25	0.543	54.6	0.997
50	0.539	64.1	0.998
100	0.534	74.2	0.997
200	0.531	84.9	0.997
500	0.528	99.9	0.997

I(t_0) = I(t_0,p). Firstly, we must pay attention to the relation between the exponent, n, and the return period, p (see Figure 2).

We have obtained Equation 13 with a very good approximation (R^2 = 0.9954):

$$n = 0.54 \left(\frac{25}{p}\right)^{0.0151 - 0.0021 \ln \frac{25}{9}} \tag{13}$$

And if we only consider return periods equal to or lower than 50 years, we obtain (R^2 = 0.96) Equation 14:

$$n \approx 0.54 \left(\frac{25}{p}\right)^{0.019 \pm 0.004} \tag{14}$$

The exponent n varies very slightly depending on the return period so, for the sake of convenience, we can view it as a constant. Thus, for IDF curves in València, we obtain n_{med} = 0.545 $\pm$ 0.015, where the interval is given by the standard deviation.

In Table 4 we can show that relative intensity $\frac{I(t_0,p)}{I(t_0,p_0)}$ is indifferent to the chosen time of reference, t_0, so we can take any other time of reference or just figure out an average of the relative intensities to eliminate possible noises.

If we represent the relation between intensity and return period, we will see in Figure 3a that it is practically insensitive to the duration t_0 taken as reference.

Taking a lineal adjustment of the logarithms (Figure 3b), we obtain a coefficient, R^2 = 0.98:

$$I(t_0, p) = I(t_0, p_0) \left(\frac{p}{p_0}\right)^{0.26 \pm 0.03} \tag{15}$$

In this case it is also insensitive to which return period is taken as reference, and we will take *I(60 min,25 y) = 52* mm h^{-1}. Logically, the larger the return period, p, is the larger the reference intensity *I(t_0,p)*.

In summary, the MAI curves of the weather in València are related to the return period p lower than 50 years, according to Equation 8 and to the following expressions:

$$n \approx n(p_0) \left(\frac{p_0}{p}\right)^{x} \tag{16}$$

$$I(t_0, p) = I(t_0, p_0) \left(\frac{p}{p_0}\right)^{m} \tag{17}$$

where for València we have obtained that:

- x = 0.019 $\pm$ 0.004
- m = 0.26 $\pm$ 0.03
- *n(25 years)* $\approx$ 0.540
- *I(60 min,25 years)* $\approx$ 52 mm h^{-1}

Given that parameter x is small, we can approximate: $n(p) \approx n_{med} \approx 0.545 \pm 0.015$, therefore, all IDF curves in València could be written as:

$$I(t, p) \approx I(t_0, p_0) \left(\frac{p}{p_0}\right)^{0.26} \left(\frac{t_0}{t}\right)^{0.545} \tag{18}$$

On the other hand, we can approximate Equation 17 to a logarithmical shape to result in:

$$I(t_0, p) \approx b(m) I_0 + a(m) I_0 \ln \frac{p}{p_0} \tag{19}$$

where $a(m) \approx 1.818m - 0.052$ and $b(m) \approx 1.0093 - 0.1479m$. Notice that with Equation 19 we obtain the approximate shape of Gumbel in Equation 5 and the approximate shape of SQRT-ET$_{max}$ in Equation 7.

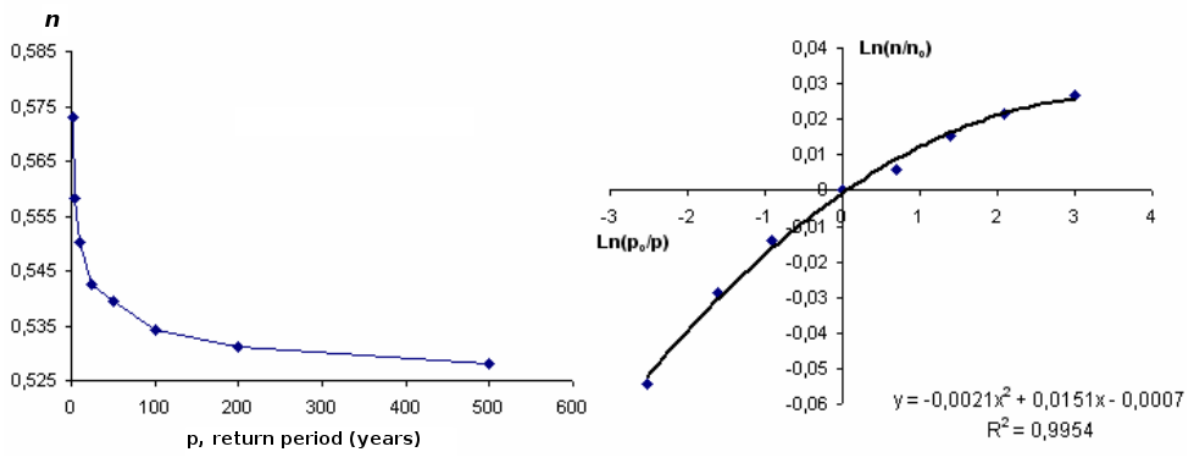

Figure 2. Relation between exponent n and return period, p, for the yearly precipitation in València, where p_0 is 25 years and n_0 is 0.543.

Table 4. Comparison of intensity and return period. The relative intensity for each duration has been taken, dividing by the corresponding intensity for a 25 years period, *I(t_0,25 years)*. Finally, the average values of all normalized intensities *I(p)/I(25 years)* have been taken for each return period, p.

	p, Return period (years)							
t_0 (minutes)	2	5	10	25 = p_0	50	100	200	500
5	0.401	0.614	0.772	1.000	1.183	1.376	1.579	1.881
10	0.447	0.645	0.794	1.000	1.170	1.340	1.532	1.794
15	0.453	0.650	0.795	1.000	1.154	1.333	1.513	1.761
20	0.480	0.670	0.810	1.000	1.170	1.330	1.510	1.750
30	0.488	0.675	0.813	1.000	1.163	1.313	1.488	1.725
60	0.454	0.650	0.795	1.000	1.167	1.336	1.522	1.788
120	0.415	0.623	0.779	1.000	1.177	1.377	1.577	1.869
180	0.400	0.613	0.771	1.000	1.187	1.384	1.594	1.892
360	0.383	0.598	0.766	1.000	1.182	1.393	1.612	1.907
720	0.391	0.602	0.766	1.000	1.188	1.391	1.609	1.914
p/p_0	0.080	0.200	0.400	1.000	2.000	4.000	8.000	20.000
$I(p)/I(p_0)$	0.431	0.634	0.786	1.000	1.174	1.357	1.554	1.828
Desv. est.	0.038	0.028	0.018	0.000	0.011	0.030	0.046	0.072

3.2 Study of a general case: IDF curves for the Iberian Peninsula

By repeating the calculations for 66 more stations of the *Agencia Estatal de Meteorología* (Spanish meteorological agency) (AEMET, 2003), we have obtained the following average values of the three adimensional parameters (see Annex B):

- x = -0.02 $\pm$ 0.02 $\approx$ 0
- m = 0.24 $\pm$ 0.03
- $n_{med} \approx 0.63 \pm 0.07$

where the indexes adjust Equations 16 and 17 and the errors are the standard deviation.

The observation of the indexes average for all 67 stations suggests that its variability is weak along the analyzed territory, so in a first approximation we could view the three indexes as constant for the whole area. In that case, we could think that the local cases of extreme precipitation would be characterized solely by the reference intensity *I(t_0,p_0)* of each station, for the same time t_0 and return period p_0.

However, if we pay attention to the values of each of the 67 stations and their error (see Annex B), the n_{med} index varies considerably from one station to another (error intervals are not compatible among themselves). Therefore, in general we will not consider it constant, but we will say that it depends on the stations considered, $n_{med} \neq$ const. The same occurs with index x, which also presents relatively very significant variations depending on the place. However, the absolute value of x is so small that it could be approximated to zero, $x \approx 0$.

Finally, the index value m presents very little variability among the places considered, with a good compatibility among the different intervals of typical error. Thus, we

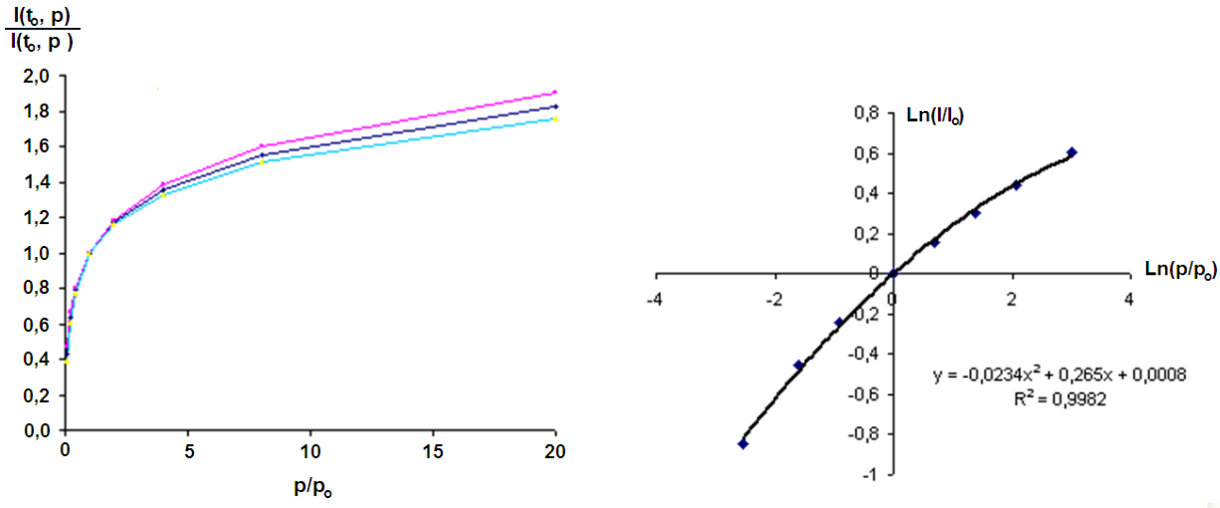

Figure 3. (a) (left) Relation between the normalized intensity I/I_0 and the normalized return period, p/p_0, of the yearly precipitation in València, for any time of reference (the two outer curves represent the typical deviation considering one time of reference or another). The reference return period taken, p_0, is 25 years. (b) (right) Logarithm of the relative intensities depending on the logarithm of the relative return period.

can consider that the average value $m = 0.24 \pm 0.03$ is a constant in the territory of interest.

Therefore, it is a good approximation to express any IDF curve of any station through a point and a parameter, that is to say, we need: (a) any reference intensity, *I(t_0,p_0)*, and (b) the average exponent n_{med}. Both values are characteristic of the local climate.

It is important to remember that the further from zero the x index is, the more variable the exponent n of a station will be. That is why one might think that, to correct this, it would be better not to dismiss the dependence of n index with the return period. However, we think that such dependence is not real, but rather a consequence of the difference of criteria when defining the IDF and MAI curves.

We must underscore that in the cases index n changed depending on the return period, it would mean that the extreme rain typology varies from convectivity to advectivity or vice versa. However, there is no clear general tendency to define the direction of this transformation according to the return period. That is to say, no standard has been observed that establishes that the extremity of a precipitation tends to move its typology to convectivity (increasing n) or advectivity (decreasing n), rather such properties respond only of the statistical domination of each local climate.

Consequently, any climatic difference in relation to the average index n_0 (associated to pluviometric extremity) represents an anomaly, by definition, and would therefore mean a local climatic variation, probably based on the wind regime, as this is the main pattern of advectivity. For all these reasons, we will continue opting for the use of the average exponent n_{med} for each station.

In conclusion, the IDF curves of each of the stations examined in this work could be written as:

$$I(t,p) \approx I(t_0,p_0)\left(\frac{p}{p_0}\right)^{0.24}\left(\frac{t_0}{t}\right)^{n_{med}} \qquad (20)$$

where *I(t,p)* is the Maximum Average Intensity depending on the duration, t, and the return period, p. While *I(t_0,p_0)* is the reference intensity, and the exponent n_{med} is characteristic of the local climatology. If we geographically represent the reference intensity for one hour and a specific period of 25 years, the result is the map in Figure 4.

Three different areas associated to the Spanish climates can be distinguished in the Iberian Peninsula. The Peninsular east and northeast stand out with reference intensities close to 60 mm h^{-1}, and in the another extreme we found Sierra Nevada and Zamora with values close to 20 mm h^{-1}.

On the other hand, if the mentioned index n_{med} for the Iberian Peninsula is represented, the result is the map in Figure 5.

IDF curves represent temporal distributions of "maximum precipitation" depending on the return period; curves that are in turn related among them as MAI curves. Therefore, the smaller the n exponent of the associated MAI is, the maximum precipitation is obtained more by persistence than by intensity, while for larger n indexes, the maximum precipitation is obtained more by intensity than by persistence. This relationship between persistence and intensity of "maximum precipitation" is reflected in climate, such that, in general, two large groups can be differentiated:

- Climates which have maximum precipitation dominated by maritime advection (zonal, northern and antizonal currents) present a lower n index, indicating a

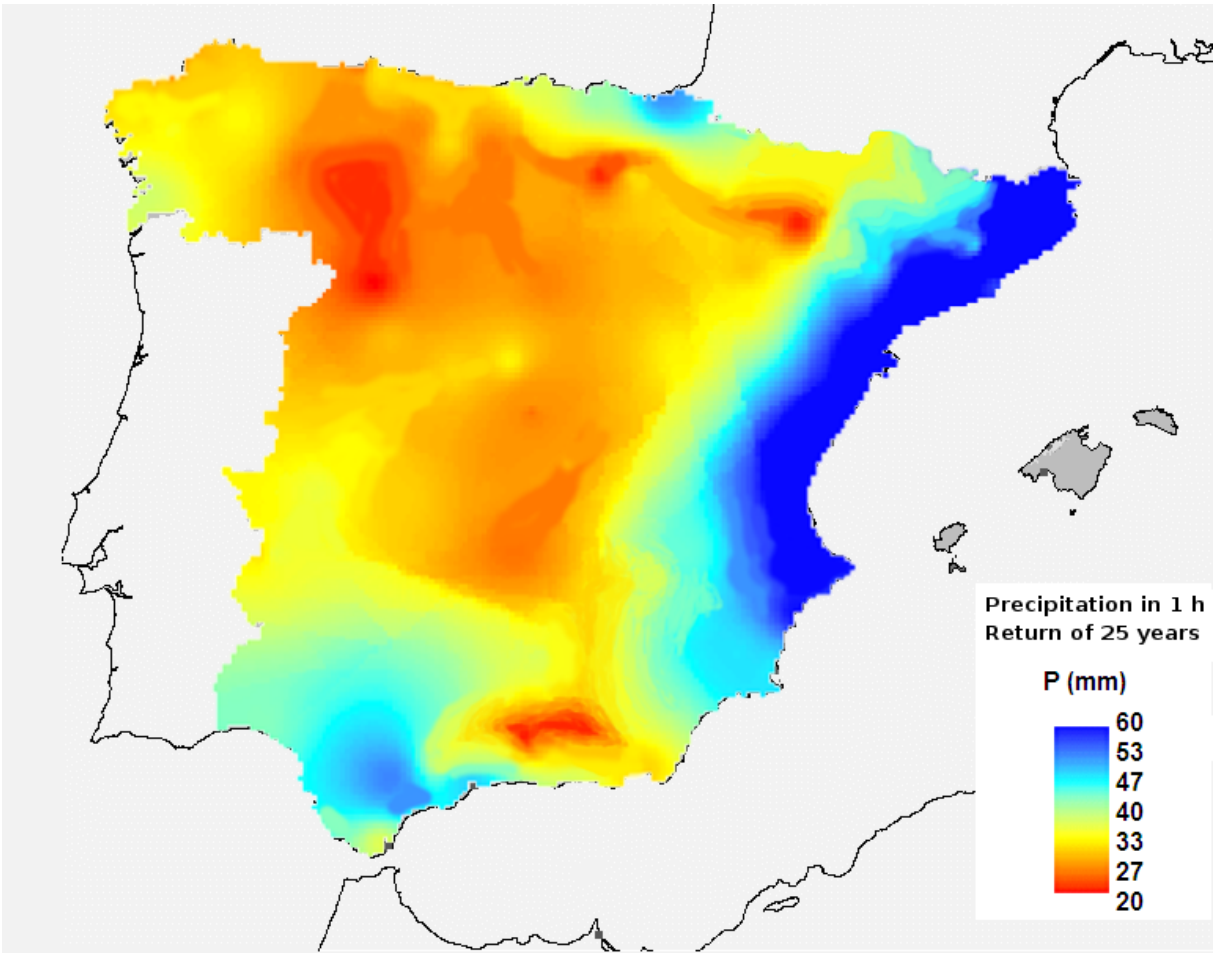

Figure 4. Maximum precipitation in one hour with a specific return period of 25 years, from the IDF curves of 67 stations of the Spanish Meteorological Agency. The map has been obtained through *kriging multivariable*, taking into consideration the distance, the regional dependences with height and distance to the sea, as well as the orientation of the slopes.

larger persistence of higher intensities. Approximately three groups can be distinguished: west half (zonal), Cantabric coast (northern) and Mediterranean coast (antizonal). Three areas with special persistence can be found in the Mediterranean coast: the gulf of València, Girona and Málaga, the three of them dominated by east winds. An area with a very low n index is found in the Cantabric coast, in the east of Asturias, which corresponds with North winds. Finally, a very important area is located in the Atlantic strip, the Central System, which presents a significant persistence in rain with the southern winds of the typical Atlantic fronts.

- Climates which have maximum precipitation dominated by convection (inland climates) present higher indexes, indicating a lower duration of maximum precipitation. There are two large areas in this situation: the east inland and the north inland of the Peninsula. Likewise, we must note that in the south of the Pyrenees, and in the northeast of the Sub-Baetic mountains there are two areas with a very high index n, which is possibly due to the scarcity of pluviometric persistence, at least during maximum precipitation.

However, there is little data available to be able to analyze both the spatial coherence by proximity and similarity, and to characterize all the regions in detail where there is no data as of yet (Pyrenees, Iberian mountains, etc.).

4 Conclusions

IDF curves of any Spanish station that is analyzed could be described in the shape of Equation 20.

There are many equivalent shapes, but this expression has advantages in relation to the others:

- It is simple. It only needs an adimensional parameter, n_{med}, and an arbitrary point $I(t_0,p_0)$.
- It contains both the dependence with the return period and the dependence of the precipitation duration.
- It is intuitive. It contains physical significance with respect to the attenuation with time, using an index be-

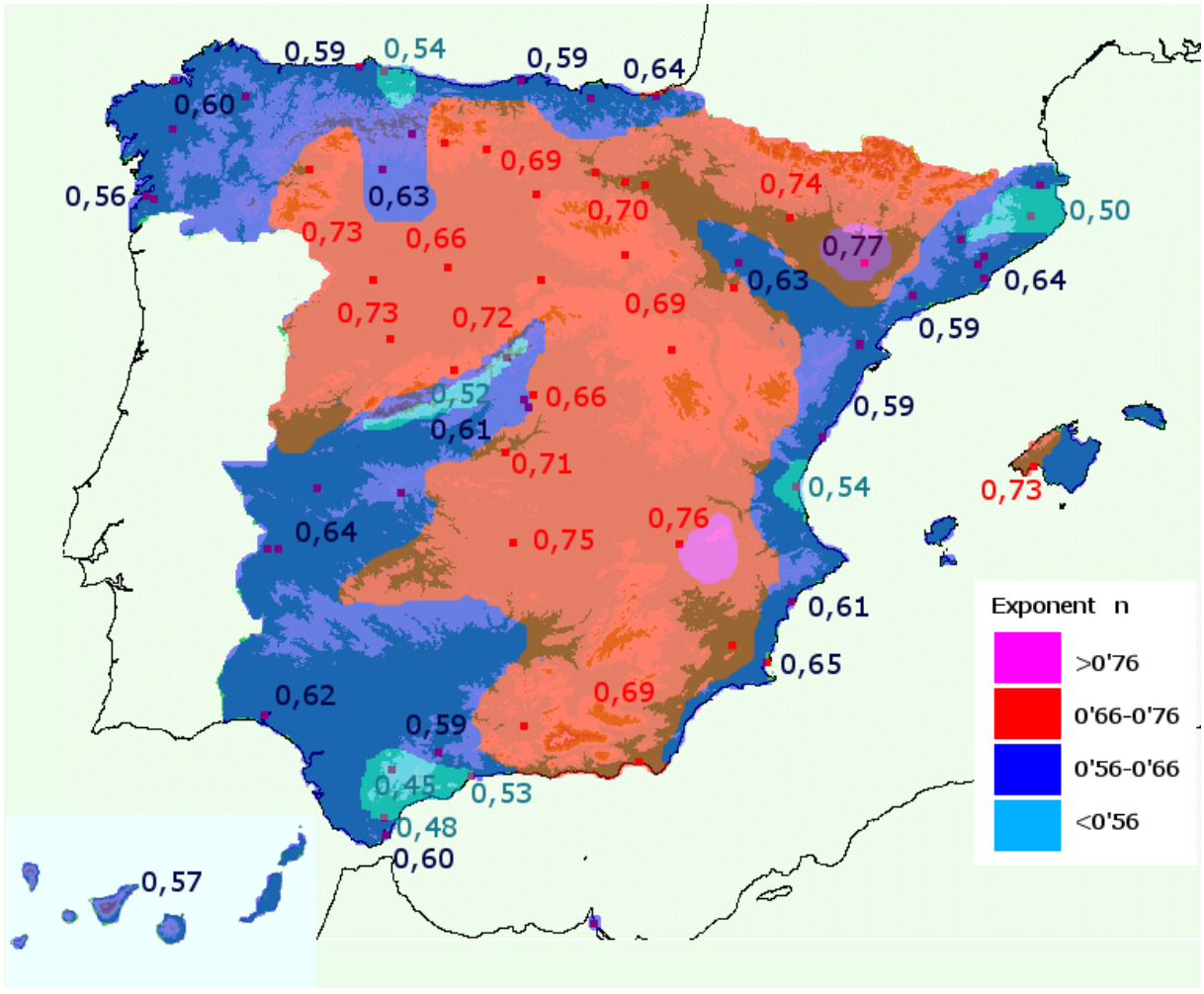

Figure 5. Distinction between climates with persistent maximum (blue) and anti-persistent (red) rainfall, from the exponent n that adjusts the IDF curves of 67 AEMET (2003) stations. The map has been obtained through *kriging multivariable*, taking into consideration the distance, the regional dependences with height and distance to the sea, as well as the orientation of the slopes.

tween 0 and 1, as well as the temporal distribution of an isolated shower.

In relation to the characteristic index n, we can distinguish between two large climate groups in the Iberian Peninsula:

- Climates which have maximum precipitation dominated by maritime advection (zonal, lateral and antizonal currents) present a lower n index, indicating a larger persistence of higher intensities. Approximately three groups can be distinguished: west half (zonal), Cantabric coast (lateral) and Mediterranean coast (antizonal).
- Climates which have maximum precipitation dominated by convection (inland climates) present higher indexes indicating a lower temporal extension of maximum precipitation.

Therefore, by the climatic definition of the relative temporal distribution index, n, associated to the local pluviometric extremity, any climatic difference regarding the average index n_o will be understood as an anomaly, that is to say, a local climatic variation, or in any case an intrinsic variability.

Acknowledgements. We want to thank the *Agencia Estatal de Meteorología* for its collaboration in making available the data of pluviometric stations, necessary to elaborate the comparative study of IDF curves. G. Chust (AZTI) is acknowledged for the revision and comments.

Appendix A Theoretical justification of the law of attenuation of Maximum Average Intensities

We want to see that the Maximum Average Intensity follows a temporal distribution this way:

$$I(t) = I_0(t_0)\left(\frac{t_0}{t}\right)^n \tag{A1}$$

where I is the MAI in a time t, I_0 is the MAI in a time of reference t_0, and n is an adimensional parameter adjustable

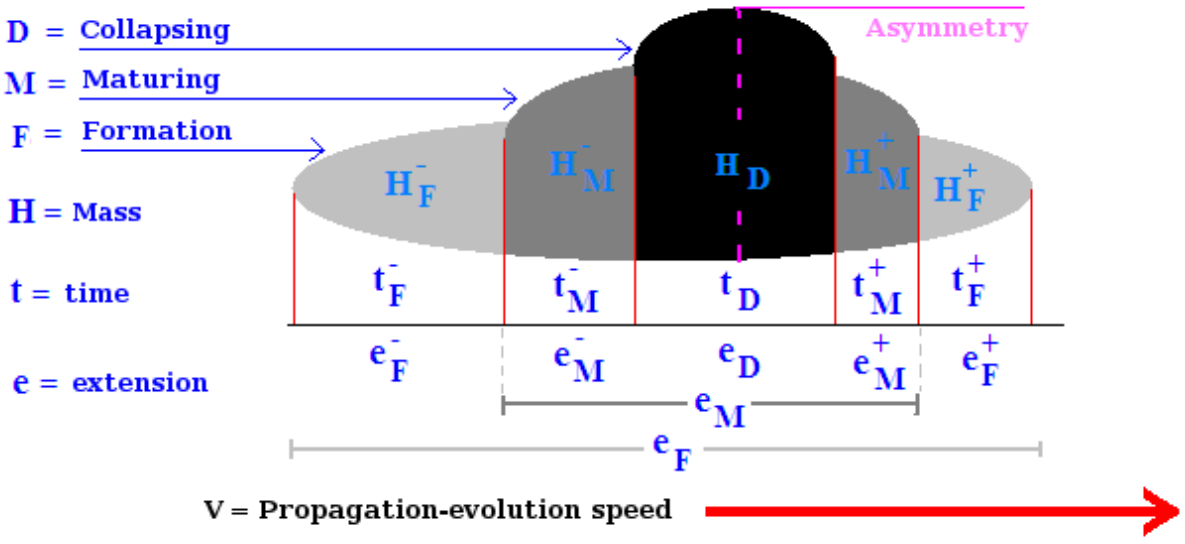

Figure A1. General diagram of a precipitating system, where P is the average precipitation associated to each level of development of the system, and e is the total extension or duration that includes the different coexisting phases of the precipitation.

to the data. Let us remember that the Maximum Average Intensity is defined as:

$$I(t) \equiv \frac{P_{max}(t)}{t} \tag{A2}$$

In order to proceed, we will use a simple diagram of a general system of intense precipitation (see Figure A1).

We can distinguish three "concentric" zones (with spatial asymmetry):

- Formation area, F: includes the whole system.
- Maturing area, M: includes intense precipitation.
- Collapsing area, D: includes the most intense focus of the system.

Logically, the total maximum precipitation, P_F (obtained in one point), is larger than the maximum precipitation during the maturing phase, P_M, and this, in turn, is larger than the maximum precipitation of the focus, P_D, as the first ones include the second ones. This is to say, $P_F = P_F^+ + P_M + P_F^-$ and $P_M = P_M^+ + P_D + P_M^-$, where $P_M^\pm$ is the maturing precipitation before and after the collapsing phase, while $P_F^\pm$ is the precipitation in the formation area, before and after the maturing area-phase. Therefore:

$$\begin{array}{l} P_D \le P_M \rightarrow I_D t_D \le I_M t_M \\ P_M \le P_F \rightarrow I_M t_M \le I_F t_F \end{array} \longrightarrow \begin{array}{l} \frac{I_D}{I_M} \le \frac{t_M}{t_D} \\ \frac{I_M}{I_F} \le \frac{t_F}{t_M} \end{array} \tag{A3}$$

where I_F is the Maximum Average Intensity in the total formation area (of a t_F duration), while I_M is the Maximum Average Intensity in the maturing area (duration t_M), and I_D is the Maximum Average Intensity in the collapsing area (t_D duration).

On the other hand, we know that the Maximum Average Intensity in the collapsing area is by definition higher than the average intensity in the maturing area, and this, in turn, is higher that the average intensity in the total formation area:

$$\begin{array}{l} I_D \le I_M \\ I_M \le I_F \end{array} \longrightarrow \begin{array}{l} 1 \le \frac{I_D}{I_M} \\ 1 \le \frac{I_M}{I_F} \end{array} \tag{A4}$$

From Equations A3 and A4, the result is that:

$$\begin{array}{l} 1 \le \frac{I_D}{I_M} \le \frac{t_M}{t_D} \\ 1 \le \frac{I_M}{I_F} \le \frac{t_F}{t_M} \end{array} \tag{A5}$$

As the times fulfill that $t_F \le t_M \le t_D$, the easiest function of the times which fulfill Equation A5 is:

$$\begin{array}{l} 1 \le \left(\frac{t_M}{t_D}\right)^n \le \frac{t_M}{t_D} \\ 1 \le \left(\frac{t_F}{t_D}\right)^n \le \frac{t_F}{t_M} \end{array} \tag{A6}$$

where n is a parameter between 0 and 1. If Equations A5 and A6 are put together, we see that it is always possible to adjust a value of n such that:

$$\begin{array}{l} \frac{I_D}{I_M} = \left(\frac{t_M}{t_D}\right)^n \\ \frac{I_M}{I_F} = \left(\frac{t_F}{t_M}\right)^n \end{array} \tag{A7}$$

Therefore, by generalizing Equation A7 for all Maximum Average Intensities, the result is:

$$\frac{I}{I_0} = \left(\frac{t_0}{t}\right)^n \tag{A8}$$

where I is the Maximum Average Intensity for an averaging time t, while I_0 is the reference intensity for an averaging time t_0, and n is an adimensional parameter between 0 and 1. It is empirically proven that the parameter n is approximately independent of the time and intensity of reference (Moncho, 2008).

Appendix B Table of the MAI adjustments to the IDF curves of a group of 67 meteorological stations with pluviograph from the Spanish meteorological agency (AEMET, 2003). The times of reference are 60 minutes for the averaging time (t_0) and 25 years for the return period (p_0)

In Table B1, $I(t_0, p_0)$ is the value of the maximum intensity directly obtained from the IDF curve for the return period p_0 and the duration t_0; while $I(t_0, p_0)'$ is the value of the maximum intensity obtained from the adjustment of MAI type carried out over the intensity values of the IDF curve, with the reference intensity for the return period p_0 and the duration t_0:

$$I(t_0, p) = I(t_0, p_0)' \left(\frac{p}{p_0}\right)^m \tag{B1}$$

where m is the exponent adjusted and tabulated in the previous table. Notice that, in theory, both values of the reference intensity should coincide in the case of a perfect adjustment (there would only be an adjustable parameter, m, which would be adimensional; since the reference intensity would be an arbitrary point in the curve, with any of the data to be adjusted).

On the other hand, $n(p_0)$ is the value of the exponent directly obtained from the adjustment of the temporal distribution of IDF curve intensities, for each return period p_0:

$$I(t) = I(t_0)\left(\frac{t_0}{t}\right)^n \rightarrow I(t, p_0) = I(t_0, p_0)\left(\frac{t_0}{t}\right)^{n(p_0)} \tag{B2}$$

That is to say, the values of $n(p_0)$ are directly identified as the exponents of the IDF curve (obtained from the adjustments of Equation B2). While $n(p_0)'$ is the value of the reference exponent which, in turn, adjusts all the exponents of IDF curves according to the expression:

$$n(p) = n(p_0)' \left(\frac{p_0}{p}\right)^x \tag{B3}$$

It should be remembered that the full expression of IDF curves is, developed from Equations B1 and B3:

$$IDF \equiv I(t, p) = I(t_0, p_0)\left(\frac{p}{p_0}\right)^m \left(\frac{t_0}{t}\right)^{n(p_0)'\left(\frac{p_0}{p}\right)^x} \tag{B4}$$

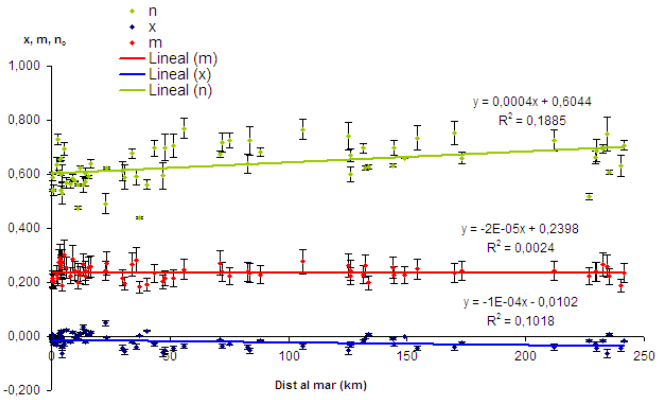

Figure B1. Comparison among the adimensional indexes of the IDF-MAI curve, depending on the distance to the sea.

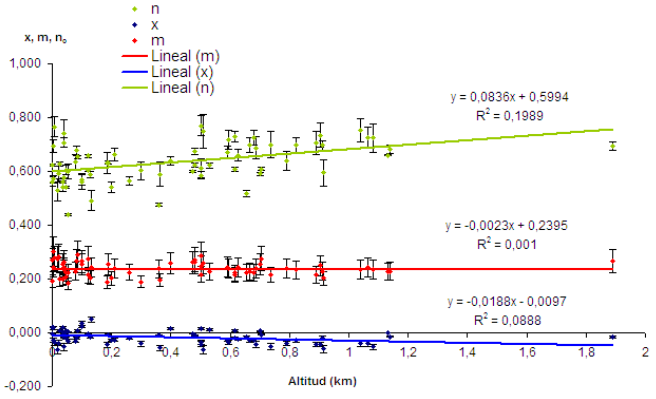

Figure B2. Comparison among the adimensional indexes of the IDF-MAI curve, depending on the height.

However, we have seen that approximately $x \approx 0$, so it is better to define an average exponent, n_{med}, that theoretically is $n_{med} = n(p_0)$, for $x = 0$. This average exponent is what we find in Equation B5:

$$I(t, p) \approx I(t_0, p_0)\left(\frac{p}{p_0}\right)^m \left(\frac{t_0}{t}\right)^{n_{med}} \tag{B5}$$

Dependence with the distance to the sea, height and latitude of the three exponential indexes n_{med}, m, x of Equations B3 and B5 has been analyzed in Figures B1, B2 and B3.

n_0 = Exponent of the adjustment of curves IDF-MAI in Equation B5, which is approximately the average exponent (independently of the return period). Notice that this is the most variable of all indexes, both regarding dispersion (strong local dependence) and regarding the variation with the considered variables (slight dependence with height and distance to the sea -Figure B2 and Figure B1-, and therefore it probably depends on the climate).

Table B1. MAI adjustments to IDF curves.

Station identifier	$I(t_0, p_0)$ IDF value	$I(t_0, p_0)$ of Equation B1	m	$\varepsilon(m)$	n_{med}	$\varepsilon(n_{med})$	$n(p_0)$ of Equation B2	$n(p_0)'$ of Equation B3	x	$\varepsilon(x)$
0034 Valls (Tarragona)	57.7	73.2	0.256	0.028	0.592	0.006	0.591	0.591	0.007	0.004
0111 Sallent Cabrianes	40.1	46.9	0.192	0.016	0.563	0.018	0.562	0.561	0.021	0.002
0201 Barcelona centro	48.4	50.9	0.276	0.032	0.657	0.006	0.658	0.658	-0.007	0.001
0222 Caldes de Montbui	59.1	75.3	0.270	0.030	0.625	0.004	0.625	0.625	-0.004	0.004
0225 Sabadell	52.6	57.6	0.259	0.028	0.643	0.015	0.641	0.641	0.016	0.006
0370 Girona	62.3	67.9	0.242	0.025	0.498	0.037	0.493	0.492	0.049	0.003
0429 Figueres	47.1	50.4	0.265	0.030	0.566	0.029	0.562	0.562	0.035	0.002
1024E San Sebastián Igueldo	43.7	45.5	0.229	0.023	0.632	0.027	0.634	0.635	-0.031	0.003
1082 Bilbao Sondica	36.2	35.8	0.242	0.025	0.574	0.002	0.574	0.575	-0.003	0.001
1110 Santander Centro	32.5	33.2	0.224	0.021	0.598	0.028	0.599	0.599	-0.032	0.002
1208 Gijón	28.6	28.2	0.207	0.019	0.544	0.005	0.542	0.541	0.007	0.004
1212 Arnao	24.3	20.2	0.205	0.018	0.590	0.012	0.589	0.587	-0.014	0.018
1387 La Coruña	25.3	24.6	0.214	0.020	0.602	0.005	0.603	0.604	-0.005	0.009
1428 Santiago Compostela	30.0	29.1	0.195	0.017	0.587	0.046	0.589	0.590	-0.056	0.008
1495 Vigo Peinador	33.1	30.5	0.225	0.021	0.563	0.016	0.564	0.565	-0.020	0.005
1496 Gondomar (Pontevedra)	29.7	33.0	0.203	0.018	0.540	0.020	0.541	0.541	-0.026	0.003
1499 Lugo punto centro	29.8	32.6	0.217	0.021	0.607	0.035	0.610	0.611	-0.042	0.004
1549 Ponferrada	23.3	22.8	0.236	0.024	0.717	0.053	0.722	0.724	-0.053	0.001
2030 Soria	26.5	27.4	0.229	0.022	0.693	0.018	0.696	0.698	-0.018	0.001
2139 Linares Arroyo (Seg.)	24.8	26.1	0.249	0.027	0.729	0.043	0.734	0.735	-0.043	0.002
2243 Pantano Aguilar (Pal.)	23.7	23.2	0.216	0.021	0.703	0.043	0.706	0.707	-0.043	0.003
2331 Burgos Villafria	26.2	27.2	0.229	0.022	0.684	0.014	0.684	0.683	-0.014	0.007
2363 Pantano Compuerto (P.)	28.4	33.3	0.216	0.021	0.693	0.050	0.697	0.699	-0.051	0.004
2422 Valladolid	24.9	24.8	0.227	0.023	0.662	0.001	0.661	0.661	0.000	0.004
2444 Ávila	28.8	32.0	0.266	0.030	0.696	0.017	0.696	0.695	-0.017	0.002
2462 Navacerrada puerto	29.7	23.9	0.225	0.022	0.517	0.012	0.518	0.518	-0.017	0.004
2614 Zamora	20.4	22.1	0.235	0.024	0.749	0.042	0.753	0.753	-0.040	0.009
2633 Pantano Porma (León)	24.1	19.8	0.202	0.019	0.591	0.049	0.595	0.596	-0.060	0.002
2661 León	21.7	19.1	0.241	0.025	0.630	0.035	0.636	0.639	-0.040	0.010
2867 Salamanca Matacán	27.3	27.2	0.242	0.025	0.721	0.040	0.724	0.725	-0.040	0.010
3013 Molina de Aragón	29.7	30.7	0.228	0.022	0.695	0.027	0.699	0.700	-0.029	0.005
3195 Madrid Retiro	25.7	26.2	0.240	0.025	0.683	0.040	0.687	0.688	-0.043	0.010
3196 Cuatro Vientos Madrid	25.3	25.7	0.222	0.021	0.609	0.008	0.609	0.609	0.008	0.001
3200 Getafe base aérea	23.9	25.4	0.241	0.025	0.658	0.024	0.662	0.664	-0.026	0.003
3259 Toledo	25.5	25.1	0.236	0.024	0.705	0.017	0.707	0.707	-0.018	0.006
3469 Cáceres	31.5	32.7	0.244	0.025	0.658	0.023	0.660	0.660	-0.025	0.014
4121 Ciudad Real	24.2	24.3	0.260	0.030	0.741	0.062	0.749	0.750	-0.063	0.010
4245 Guadalupe (Cáceres)	27.5	19.6	0.188	0.017	0.627	0.040	0.630	0.631	-0.045	0.009
4452 Talavera (Badajoz)	31.8	32.9	0.256	0.027	0.630	0.007	0.632	0.632	-0.008	0.009
4478 Badajoz	28.5	30.7	0.198	0.017	0.628	0.007	0.628	0.629	0.008	0.002
4605 Huelva	36.8	42.2	0.227	0.022	0.621	0.010	0.621	0.622	0.010	0.007
5530 Granada	20.6	20.4	0.234	0.024	0.694	0.028	0.696	0.696	-0.028	0.005
5911 Grazalema	43.5	38.9	0.183	0.015	0.442	0.003	0.441	0.440	0.004	0.007
6000A Melilla	35.5	37.2	0.255	0.027	0.573	0.019	0.570	0.570	0.023	0.011
6006 Algeciras	31.6	34.6	0.190	0.016	0.601	0.035	0.602	0.602	-0.040	0.003
6024 Pan. Guadarranque	33.4	32.2	0.238	0.024	0.474	0.006	0.476	0.476	-0.009	0.010
6120 Pan. Guadalhorce (Ma)	32.1	29.6	0.284	0.033	0.583	0.029	0.589	0.591	-0.038	0.015
6172 Málaga 'jardín observ.'	42.3	46.9	0.275	0.032	0.523	0.043	0.530	0.531	-0.062	0.006
6325O Almería	29.0	32.5	0.301	0.038	0.689	0.024	0.693	0.694	-0.026	0.007
7031 San Javier	41.5	44.5	0.291	0.035	0.654	0.007	0.653	0.653	0.007	0.004
7228 Alcantarilla (Murcia)	41.3	44.6	0.266	0.029	0.676	0.018	0.678	0.678	-0.020	0.001
8025 Alicante	50.4	55.7	0.275	0.032	0.606	0.006	0.608	0.608	-0.007	0.002
8175 Albacete	39.1	38.6	0.277	0.032	0.760	0.037	0.765	0.765	-0.036	0.002
8416 València	54.6	51.9	0.255	0.028	0.545	0.015	0.543	0.541	0.019	0.006
8500A Castelló	60.1	71.4	0.262	0.028	0.602	0.004	0.602	0.602	-0.005	0.001
9121 Haro (La Rioja)	21.3	21.9	0.272	0.031	0.674	0.012	0.674	0.673	-0.013	0.009
9148 Logroño	28.3	29.6	0.240	0.025	0.712	0.035	0.717	0.719	-0.035	0.009
9171 Cabreja (Navarra)	24.3	21.2	0.225	0.022	0.723	0.027	0.725	0.726	-0.026	0.004
9434 Zaragoza aeropuerto	28.0	28.4	0.263	0.029	0.623	0.008	0.624	0.625	-0.008	0.011
9443 Pan. Mezalocha (Zar.)	30.1	29.5	0.244	0.026	0.666	0.024	0.670	0.671	-0.026	0.004
9771 Lleida	40.1	43.7	0.248	0.026	0.764	0.037	0.768	0.770	-0.035	0.007
9898 Huesca Monflorite	21.2	19.1	0.262	0.030	0.730	0.051	0.738	0.740	-0.053	0.011
9980 Tortosa (Tarragona)	56.4	67.4	0.225	0.022	0.602	0.018	0.604	0.605	-0.021	0.004
9981A Tortosa Roquetas	53.6	58.4	0.243	0.025	0.573	0.015	0.571	0.571	0.018	0.015
B228 Palma ciudad	33.2	37.5	0.215	0.021	0.728	0.020	0.729	0.729	-0.019	0.002
C447A Tenerife N. Rodeos	28.3	25.2	0.200	0.018	0.562	0.005	0.562	0.561	0.005	0.009
C449C Sta. Cruz de Tenerife	29.4	29.9	0.288	0.035	0.586	0.013	0.585	0.586	0.016	0.003
Media	33.9	31.7	0.239	0.025	0.633	0.023	0.634	0.635	-0.018	0.931
Desviación típica	11.0	10.2	0.027	0.005	0.072	0.015	0.073	0.074	0.025	0.116

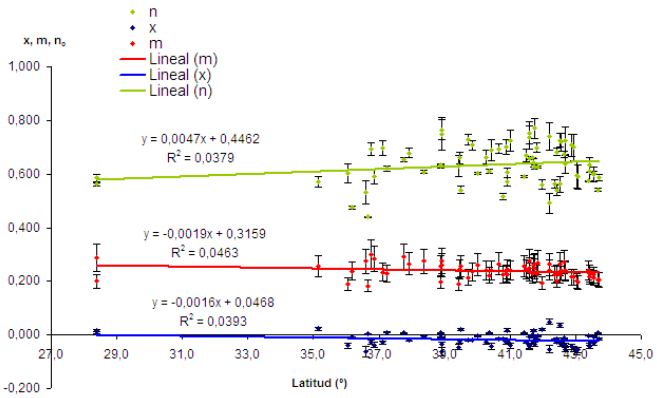

Figure B3. Comparison among the adimensional indexes of the IDF-MAI curve, depending on the latitude.

m = Exponent of the return periods. In this case, the dependence with any geographical parameter is virtually nil. From this we deduce that m is constant, at least in the considered territory, and the observed variability is probably due to noise conditioned to the data (see Figure B1, Figure B2 and Figure B3).

x = Exponent of the variability of n regarding the return periods. In this case there is also a little variation with regard to the climate, but in any case is x close to 0, and therefore it can be dismissed (see Figure B1, Figure B2 and Figure B3).

References

AEMET, 2003: CURVAS de intensidad - duración - frecuencia [Archivo de ordenador]: Estructura temporal de la precipitación, AEMET, Madrid, 1 disco compacto; 12 cm. D. L. M. 53200-03. ISBN 84-8320-258-1.

Chow, V. T., 1962: Hydrologic determination of waterway areas for drainage structures in small drainage basins, Engrg. Experimental Station, Univ. of Illinois, Urbana, I11, Illinois, bulletin No. 462.

Etoh, T., Murota, A., and Nakanishi, M., 1986: SQRT-Exponential Type Distribution of Maximum, Hydrologic Frequency Modelling, V. P. Shing (ed.), Reidel Pub. Com. U.S.A., Lousiana State University, proceedings of the International Symposium on Flood Frequency and Risk Analyses, 14-17 May 1986, pp. 253-264.

Ferrer, F. J., 1996: El modelo de función de distribucin SQRT-ET max en el análisis regional de máximos hidrológicos : aplicación a lluvias diarias, Tesis Doctoral, Universidad Politécnica de Madrid.

Ghahraman, B. and Hoss Eini, S. M., 2005: *A new investigation on the perforance of rainfall IDF models*, Iran J Sci Technol Trans B-Eng, **29**.

Moncho, R., 2008: *Análisis de la intensidad de precipitación. Método de la intensidad contigua*, RAM3, **Enero**.

M.O.P.U., 1990: Unidades hidrogeológicas de la España peninsular e Islas Baleares, Informaciones y estudios n° 52. Servicio Geológico, Madrid.

NASA, 2008: *Global Temperature Trends: 2007 Summation*, DATASETS & IMAGES in GISS Surface Temperature Analysis.

NOAA, 2008: *Climate of 2007 Annual Report*, National Climatic Data Center, **15 January**.

Pereyra-Díaz, D., Pérez-Sesma, J. A. A., and Gómez-Romero, L., 2004: *Ecuaciones que estiman las curvas Intensidad-Duración-Período de retorno de la lluvia*, GEOS, **24**, 46–56.

Remenieras, G., 1970: L'Hydrologie de L'ingénieur. Collection du Recherches et D'essais de Chatou, Water Affair Publication, Ministry of Energy, 1, 383, translated to Persian by: H. Sedghi.

Sherman, C., 1931: *Frequency and intensity of excessive rainfall at Boston, Massachusetts*, Transactions, American Society of Civil Engineers, **95**, 951–960.

Témez, J., 1978: Cálculo Hidrometeorológico de caudales máximos en pequeñas cuencas naturales, Dirección General de Carreteras, Madrid, p. 111.